Dimension reduction analysis with mapping and direct integration algorithm

J.Jin[1], T Huang[1], J.L. Zheng[1] and P.H. Wen[*2]

[1]*School of Traffic and Transportation Engineering, Changsha University of Technology and Science, China*

[2]*School of Engineering and Materials Science, Queen Mary, University of London, London E1 4NS, UK*

Abstract

Based on the Lagrange series interpolation, the semi-analytical and direct integration method (DIM) for solving the multi-dimensional partial differential equations are presented in this paper. A multidimensional problem can be simplified to a set of the ordinary differential equation by the mapping technique and Lagrange series interpolation (dimension reduction). The semi-analytical and numerical solutions by DIM are derived for the partial differential equation with variable coefficients. Comparisons with analytical solutions are performed in order to demonstrate the accuracy and efficiency of the proposed method.

Key words: multi-dimensional partial differential equations, semi-analytical solution, finite difference method, Laplace transform, dynamics, functionally graded materials.

*Corresponding author: p.h.wen@qmul.ac.uk, Tel: 44 20 7882 5371

1. Introduction

Most problems in engineering end up with solving a set of multi-dimensional partial differential equations (PDEs) by using modelling techniques. For potential problems, the Poisson type differential equation is to be solved either analytically or numerically. Due to the high performance of computers, the numerical approximations can usually provide a high degree of accuracy together with a reliable bound on the error with the analytical solution. There are many numerical techniques to deal with differential equations including the semi-analytical solutions, the finite difference method, finite element method and boundary element method in [1-6]. In the last decade, high performance of interpolation by using the radial basis functions and Lagrange series interpolation have been drawing a great attention of researchers, see Golberg et. al. [7], Hardy [8] and Hon et. al. [9]. Recently the meshless approaches in the numerical engineering including the Diffuse Element Method (DEM), Element-Free Galerkin (EFG), Finite Point Method, Meshless Local Petrov-Galerkin (MLPG) and Point Interpolation Method (PIM) [10-14] etc have received much interest since Nayroles et. al. [15] proposed the diffuse element method. The scaled boundary finite element method has been developed in [16] which was extended to solve problems in diffusion [17], dynamic fluid-structure interaction [18] and acoustics [19]. Stress intensity factors are evaluated in [20] for cracks with the crack surfaces subjected to arbitrarily distributed tractions. The finite integration method and finite block method developed by Wen et. al. [21,22] and Li et. al. [23] were applied to engineering problems including fracture mechanics, heat conductivity, nonlinear contact static and dynamic problems. It shows that the FIM provide much higher accuracy degree than the finite difference method and the point collocation method.

In this paper, the Finite Line Integration Method is proposed to deal with multi-dimensional partial differential equations. Firstly, the real domain is mapped into a square domain first and the partial differential equation is derived in the normalized domain. The Lagrange series interpolation is applied to $D-1$ coordinate axis for multi-dimensions (D is the dimension number). Then the partial differential equation is reduced to a set of ordinary differential equations. Two numerical approaches are employed to solve the ordinary differential equation, i.e. the finite difference approach and finite integration approach. To demonstrate the accuracy

and efficiency of the DIM, two-dimensional problems are observed and the numerical results are compared with analytical solutions.

2. Coordinate transform and mapping differential matrix

2.1. Two dimensional problem

For a two dimensional problem, suppose that the domain shown in Figure 1(a) is mapped into a square domain by using the following shape functions for the geometry [24]

$$M_i = \frac{1}{4}(1+\xi_i\xi)(1+\eta_i\eta)(\xi_i\xi+\eta_i\eta-1) \quad \text{for} \quad i=1,2,3,4,$$

$$M_i = \frac{1}{2}(1-\xi^2)(1+\eta_i\eta) \quad \text{for} \quad i=5,7, \tag{1}$$

$$M_i = \frac{1}{2}(1-\eta^2)(1+\xi_i\xi) \quad \text{for} \quad i=6,8,$$

where (ξ_i,η_i) indicates seed coordinate in regular domain. The different order of partial differentials of shape function with respect to axes ξ and η are presented in the Appendix. The coordinate in a real domain is interpolated as

$$x=\sum_{k=1}^{8} M_k(\xi,\eta)x_k,\ \ y=\sum_{k=1}^{8} M_k(\xi,\eta)y_k\,. \tag{2}$$

For the first order partial differentials of function $u(x,y)$ in Cartesian coordinates, one has

$$\frac{\partial u}{\partial x}=\alpha_{11}\frac{\partial u}{\partial \xi}+\alpha_{12}\frac{\partial u}{\partial \eta},\ \ \frac{\partial u}{\partial y}=\alpha_{21}\frac{\partial u}{\partial \xi}+\alpha_{22}\frac{\partial u}{\partial \eta}, \tag{3}$$

where

$$\alpha_{11}=\frac{1}{J}\frac{\partial y}{\partial \eta},\alpha_{12}=-\frac{1}{J}\frac{\partial y}{\partial \xi},\alpha_{21}=-\frac{1}{J}\frac{\partial x}{\partial \eta},\alpha_{22}=\frac{1}{J}\frac{\partial x}{\partial \xi},\ \ J=\begin{vmatrix}\dfrac{\partial x}{\partial \xi} & \dfrac{\partial x}{\partial \eta}\\ \dfrac{\partial y}{\partial \xi} & \dfrac{\partial y}{\partial \eta}\end{vmatrix}.$$

Therefore, the second order partial differentials can be written, from (3), as

$$\frac{\partial^2 u}{\partial x^2}=\frac{\partial \alpha_{11}}{\partial x}\frac{\partial u}{\partial \xi}+\alpha_{11}\frac{\partial^2 u}{\partial x\partial \xi}+\frac{\partial \alpha_{12}}{\partial x}\frac{\partial u}{\partial \eta}+\alpha_{12}\frac{\partial^2 u}{\partial x\partial \eta}$$

$$=\frac{\partial u}{\partial \xi}\left[\alpha_{11}\frac{\partial \alpha_{11}}{\partial \xi}+\alpha_{12}\frac{\partial \alpha_{11}}{\partial \eta}\right]+\alpha_{11}\left[\alpha_{11}\frac{\partial^2 u}{\partial \xi^2}+\alpha_{12}\frac{\partial^2 u}{\partial \xi\partial \eta}\right] \tag{4}$$

$$+\frac{\partial u}{\partial \eta}\left[\alpha_{11}\frac{\partial \alpha_{12}}{\partial \xi}+\alpha_{12}\frac{\partial \alpha_{21}}{\partial \eta}\right]+\alpha_{12}\left[\alpha_{11}\frac{\partial^2 u}{\partial \xi \partial \eta}+\alpha_{12}\frac{\partial^2 u}{\partial \eta^2}\right]$$

$$\frac{\partial^2 u}{\partial x \partial y}=\frac{\partial \alpha_{11}}{\partial y}\frac{\partial u}{\partial \xi}+\alpha_{11}\frac{\partial^2 u}{\partial y \partial \xi}+\frac{\partial \alpha_{12}}{\partial y}\frac{\partial u}{\partial \eta}+\alpha_{12}\frac{\partial^2 u}{\partial y \partial \eta}$$

$$=\frac{\partial u}{\partial \xi}\left[\alpha_{21}\frac{\partial \alpha_{11}}{\partial \xi}+\alpha_{22}\frac{\partial \alpha_{11}}{\partial \eta}\right]+\alpha_{11}\left[\alpha_{21}\frac{\partial^2 u}{\partial \xi^2}+\alpha_{22}\frac{\partial^2 u}{\partial \xi \partial \eta}\right] \tag{5}$$

$$+\frac{\partial u}{\partial \eta}\left[\alpha_{21}\frac{\partial \alpha_{12}}{\partial \xi}+\alpha_{22}\frac{\partial \alpha_{21}}{\partial \eta}\right]+\alpha_{12}\left[\alpha_{21}\frac{\partial^2 u}{\partial \xi \partial \eta}+\alpha_{22}\frac{\partial^2 u}{\partial \eta^2}\right]$$

and

$$\frac{\partial^2 u}{\partial y^2}=\frac{\partial \alpha_{21}}{\partial y}\frac{\partial u}{\partial \xi}+\alpha_{21}\frac{\partial^2 u}{\partial y \partial \xi}+\frac{\partial \alpha_{22}}{\partial y}\frac{\partial u}{\partial \eta}+\alpha_{22}\frac{\partial^2 u}{\partial y \partial \eta}$$

$$=\frac{\partial u}{\partial \xi}\left[\alpha_{21}\frac{\partial \alpha_{21}}{\partial \xi}+\alpha_{22}\frac{\partial \alpha_{21}}{\partial \eta}\right]+\alpha_{21}\left[\alpha_{21}\frac{\partial^2 u}{\partial \xi^2}+\alpha_{22}\frac{\partial^2 u}{\partial \xi \partial \eta}\right] \tag{6}$$

$$+\frac{\partial u}{\partial \eta}\left[\alpha_{21}\frac{\partial \alpha_{22}}{\partial \xi}+\alpha_{22}\frac{\partial \alpha_{22}}{\partial \eta}\right]+\alpha_{22}\left[\alpha_{21}\frac{\partial^2 u}{\partial \xi \partial \eta}+\alpha_{22}\frac{\partial^2 u}{\partial \eta^2}\right].$$

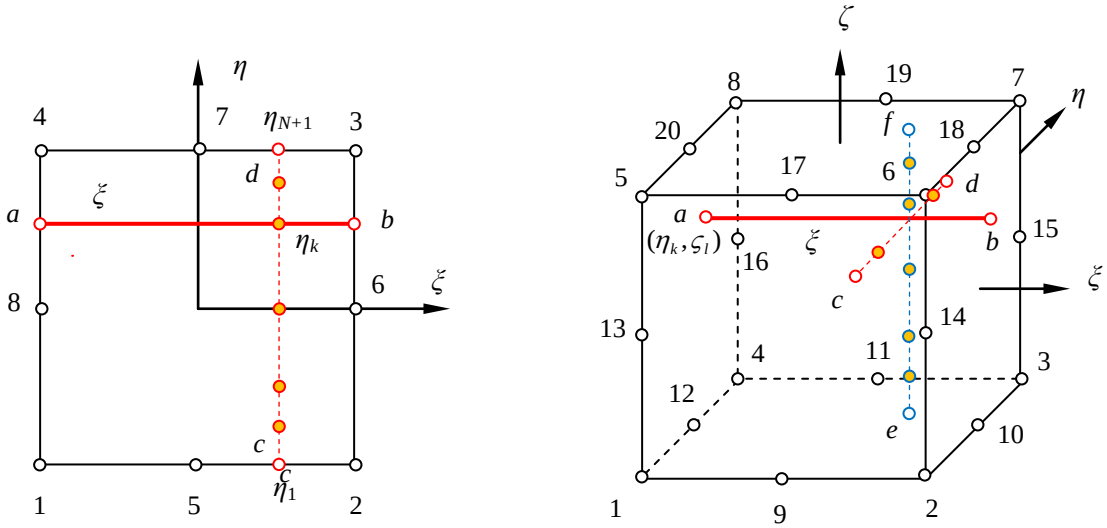

(a) (b)

Figure 1. Regular domain and its seeds: (a) two dimension; (b) three dimension.

Consider a Poisson equation for two-dimensional problems

$$\frac{\partial^2 u}{\partial x^2}+\frac{\partial^2 u}{\partial y^2}=b(x,y) \quad (x,y)\in\Omega, \tag{7}$$

where $b(x,y)$ is source term in the domain and Ω. The equation above in the normalised transformed domain becomes

$$\frac{\partial^2 u}{\partial \xi^2}+A\frac{\partial u}{\partial \xi}+B\frac{\partial u}{\partial \eta}+C\frac{\partial^2 u}{\partial \xi\partial \eta}+D\frac{\partial^2 u}{\partial \eta^2}=Eb(\xi,\eta), \tag{8}$$

where

$$\begin{aligned}
A&=\left(\alpha_{11}\frac{\partial\alpha_{11}}{\partial\xi}+\alpha_{12}\frac{\partial\alpha_{11}}{\partial\eta}+\alpha_{21}\frac{\partial\alpha_{21}}{\partial\xi}+\alpha_{22}\frac{\partial\alpha_{21}}{\partial\eta}\right)/\left(\alpha_{11}^2+\alpha_{21}^2\right),\\
B&=\left(\alpha_{11}\frac{\partial\alpha_{12}}{\partial\xi}+\alpha_{12}\frac{\partial\alpha_{12}}{\partial\eta}+\alpha_{21}\frac{\partial\alpha_{22}}{\partial\xi}+\alpha_{22}\frac{\partial\alpha_{22}}{\partial\eta}\right)/\left(\alpha_{11}^2+\alpha_{21}^2\right),\\
C&=2\left(\alpha_{11}\alpha_{12}+\alpha_{22}\alpha_{21}\right)/\left(\alpha_{11}^2+\alpha_{21}^2\right),\\
D&=\left(\alpha_{12}^2+\alpha_{22}^2\right)/\left(\alpha_{11}^2+\alpha_{21}^2\right),\ E=1/\left(\alpha_{11}^2+\alpha_{21}^2\right).
\end{aligned} \tag{9}$$

The first and second order partial differentials of coefficients α_{ij} with respect to axes ξ and η are given in the Appendix.

2.2. Dimension reduction (2D)

For two dimensional problems, suppose that the real domain shown in Figure 1(a) has four edges associated with $\xi=\pm1,\ \eta=\pm1$. The boundary conditions can be written in general form as

$$f_i(\xi_0,\eta_0)u+g_i(\xi_0,\eta_0)\frac{du}{dn}=w_i(\xi_0,\eta_0)\quad i=1,2,3,4 \quad (\xi_0,\eta_0)\in\partial\Omega, \tag{10}$$

in which f_i, g_i and w_i are given functions on the boundary $\partial\Omega$, i indicates the numbers of edge and n is the outward normal to the boundary. From the coordinate transform, one has

$$\frac{du}{dn}=\frac{du}{dx}\cos\alpha+\frac{du}{dy}\sin\alpha=\left(\alpha_{11}\cos\alpha+\alpha_{21}\sin\alpha\right)\frac{\partial u}{\partial\xi}+\left(\alpha_{12}\cos\alpha+\alpha_{22}\sin\alpha\right)\frac{\partial u}{\partial\eta}. \tag{11}$$

In the mapped domain, the potential function can be interpolated by using Lagrange series along a straight line *cd* in Figure 1(a) as follows

$$u(\xi,\eta)=\sum_{n=1}^{N}\prod_{\substack{k=1\\k\neq n}}^{N}\frac{(\eta-\eta_k)}{(\eta_n-\eta_k)}u_n(\xi)=\sum_{n=1}^{N}N_n(\eta)\,u_n(\xi), \tag{12}$$

where $N_n(\eta)$ is also called as the shape function with Lagrange series interpolation along line *cd* and the collocations of distributed nodes are selected either uniformly as

$$\eta_k=-1+\frac{2(k-1)}{N},\ k=1,2,...,N+1, \tag{13}$$

or non-uniformly distribution such as Chebyshev's roots

$$\eta_k=-\cos\frac{\pi(k-1)}{N},\ k=1,2,...,N+1. \tag{14}$$

It is very clear that the selection of collocation with Chebyshev's roots gives a much stable and accurate solution in general cases [24]. Then the first order and second order derivatives with respect to coordinate η are obtained easily as

$$\frac{\partial u}{\partial \eta}=\sum_{i=1}^{N}\left[\prod_{k=1,k\neq i}^{N}(\eta_i-\eta_k)^{-1}\sum_{j=1}^{N}\prod_{k=1,k\neq i,k\neq j}^{N}(\eta-\eta_k)\right]u_i(\xi)=\sum_{i=1}^{N}\frac{dN_i(\eta)}{d\eta}u_i(\xi) \tag{15}$$

and

$$\frac{\partial^2 u}{\partial \eta^2}=\sum_{i=1}^{N}\left[\prod_{k=1,k\neq i}^{N}(\eta_i-\eta_k)^{-1}\sum_{l=1}^{N}\sum_{j=1,j\neq l}^{N}\prod_{k=1,k\neq i,k\neq j,k\neq l}^{N}(\eta-\eta_k)\right]u_i(\xi)=\sum_{i=1}^{N}\frac{d^2N_i(\eta)}{d\eta^2}u_i(\xi). \tag{16}$$

Substituting (15) and (16) into (10) gives

$$\frac{\partial^2 u}{\partial \xi^2}+A\frac{\partial u}{\partial \xi}+B\sum_{i=1}^{N}\frac{\partial N_i(\eta)}{\partial \eta}u_i(\xi)+C\sum_{i=1}^{N}\frac{\partial N_i(\eta)}{\partial \eta}\frac{\partial u_i(\xi)}{\partial \xi}+D\sum_{i=1}^{N}\frac{\partial^2 N_i(\eta)}{\partial \eta^2}u_i(\xi)=Eb(\xi,\eta). \tag{17}$$

If we consider a straight line $\eta=\eta_k$ shown in Figure 1(a) in the domain, the partial differential equation becomes an ordinary differential equation as

$$\frac{d^2u_k}{d\xi^2}+A\frac{du_k}{d\xi}+B\sum_{i=1}^{N}\frac{dN_i(\eta_k)}{d\eta}u_i(\xi)+C\sum_{i=1}^{N}\frac{dN_i(\eta_k)}{d\eta}\frac{du_i(\xi)}{d\xi}+D\sum_{i=1}^{N}\frac{d^2N_i(\eta_k)}{d\eta^2}u_i(\xi)=Eb(\xi,\eta_k)$$
$$k=2,....,N-1, \tag{18}$$

where *N*+1 is the number of collocation point in total along the η axis. Apparently, the problem with the partial differential equation is changed to solve an ordinary differential equation with a set of the distribution function $u_i(\xi)$. Similar to the scaled boundary finite element method [16], this approach aims to simply transfer a partial differential equation to an ordinary differential equation and is therefore defined as the direct integration method. It is

expected to be easier and more accurate to deal with an ordinary differential equation than a partial differential equation.

2.3. Dimension reduction (3D)

This dimension reduction method can be easily extended to a three dimensional problem. In three-dimensional cases, the real domain is associated with six surfaces, i.e. $\xi = \pm 1$, $\eta = \pm 1$, $\varsigma = \pm 1$ with the following boundary conditions

$$f_i(\xi_0, \eta_0, \varsigma_0)u + g_i(\xi_0, \eta_0, \varsigma_0)\frac{du}{dn} = w_i(\xi_0, \eta_0, \varsigma_0) \quad i = 1,2,3,4,5,6, \quad (\xi_0, \eta_0, \varsigma_0) \in \partial\Omega, \tag{19}$$

in which f_i, g_i and w_i are specified on the boundary $\partial\Omega$ as shown in Figure 1(b). In the mapped domain, similarly to two-dimensional problems, the potential function can be interpolated by using Lagrange series, along line *ef* in Figure 2(b), as follows

$$u(\xi, \eta, \varsigma) = \sum_{n=1}^{N}\prod_{\substack{k=1 \\ k\neq i}}^{N}\frac{(\eta - \eta_k)}{(\eta_n - \eta_k)}\sum_{l=1}^{L}\prod_{\substack{j=1 \\ j\neq l}}^{L}\frac{(\varsigma - \varsigma_j)}{(\varsigma_l - \varsigma_j)}u_{nl}(\xi) = \sum_{i=1}^{N}\sum_{l=1}^{L}N_n(\eta)\,L_l(\varsigma)u_{nl}(\xi), \tag{20}$$

where $N_n(\eta)$ and $L_l(\varsigma)$ are shape functions along η and ς axis respectively. In the same way for 2D problems, the first order and second order derivatives with respect to coordinate η and ς can be obtained easily by Lagrange interpolation. Therefore, a three-dimension partial differential equation can be transformed to a set of the ordinary differential equation.

3. Semi-analytical and direct integration algorithm

In order to investigate the degree of accuracy, the semi-analytical analysis is presented in this section. Consider a Laplace differential equation with regular domain $|x| \le 1$, $|y| \le 1$

$$\frac{\partial^2 u}{\partial x^2} + \frac{\partial^2 u}{\partial y^2} = 0. \tag{21}$$

In this case, $x = \xi$, $y = \eta$, $A = B = C = 0$ and $D = E = 1$. By Lagrange series interpolation and considering a straight line $y = y_k$ shown in Figure 2(a), the partial differential equation is simplified to the ordinary differential equation as follow

$$\frac{d^2u_k}{dx^2}+\sum_{n=1}^{N+1}\frac{d^2N_n(y_k)}{dy^2}u_n(x)=0\,,\quad y=y_k\,,\quad k=2,....,N\,. \tag{22}$$

Suppose on the top and bottom $u=0$ when $y=\pm1$, i.e. $u_1(x)=u_{N+1}(x)=0$ and the general solution of the potential can be written as

$$u_k(x)=\beta_k e^{\lambda x}\quad k=2,....,N\,, \tag{23}$$

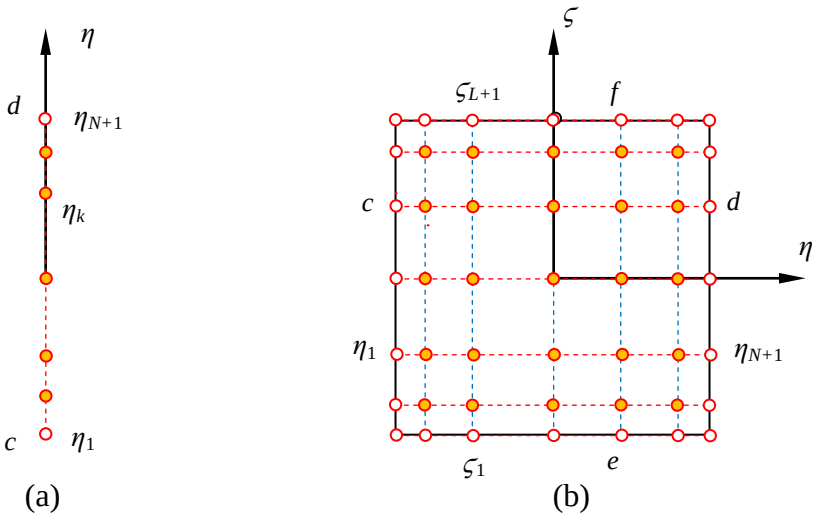

Figure 2. Ends for each integration line: ○boundary nodes; ● domain nodes: (a) two dimension; (b) three dimension.

where β_k are coefficients. Substituting (23) into (22) gives

$$\beta_k\lambda^2+\sum_{n=2}^{N}\frac{d^2N_n(y_k)}{dy^2}\beta_n=0\qquad k=2,....,N\,. \tag{24}$$

Then, the general solution of Eq.(22) can be written as

$$\mathbf{u}(x)=\left(u_2,u_3,...,u_N\right)^T=\sum_{k=2}^{N}\beta_k e^{\sqrt{\lambda_k}x}\mathbf{v}_k+\sum_{k=2}^{N}\overline{\beta}_k e^{-\sqrt{\lambda_k}x}\overline{\mathbf{v}}_k\,, \tag{25}$$

where λ_k and $\mathbf{v}_k=\left\{v_{k2},v_{k3},...,v_{kN}\right\}^T$ represent the eigenvalues and associated eigenvectors of the following equations in matrix form

$$\left(\mathbf{K}-\lambda\mathbf{I}\right)\mathbf{v}=0\,, \tag{26}$$

where $K_{kn} = -\dfrac{d^2 N_n(y_k)}{dy^2}$ and $\mathbf{I}$ is $(N-1)\times(N-1)$ diagonal unite matrix, β_i and $\overline{\beta}_i$ are coefficients to be determined by boundary conditions at the ends of each line shown in Figure 2(a)(b), i.e. when $x = \pm 1$ and $y = y_k$ in (22). In the same way, for three-dimensional cases shown in Figure 2(b), the Laplace equation is

$$\frac{d^2 u_{kj}(x)}{dx^2} + \sum_{n=1}^{N+1} \frac{d^2 N_n(y_k)}{dy^2} u_{nj}(x) + \sum_{l=1}^{L+1} \frac{d^2 L_l(z_j)}{dz^2} u_{kl}(x) = 0, \quad y = k_k, z = z_j$$

$$k = 2,....,N, \ \ j = 2,....,L. \tag{27}$$

Suppose $u = 0$ when $y = 0,1$ and $z = 0,1$, and the general solution of the ordinary differential equation above can be written as

$$u_{kj}(\xi) = \beta_{kj} e^{\lambda \xi}, \ \ k = 2,....,N, \ \ j = 2,....,L, \tag{28}$$

where β_{kj} is coefficients. Substituting (28) into (27) yields

$$\beta_{kj}\lambda^2 + \sum_{n=2}^{N} \frac{d^2 N_n(y_k)}{dy^2} \beta_{nj} + \sum_{l=2}^{L} \frac{d^2 N_l(z_j)}{dz^2} \beta_{kl} = 0, \quad k = 2,....,N, \ \ j = 2,....,L. \tag{29}$$

It is a set of ordinary differential equations and their general solutions can be obtained as

$$\mathbf{u}(x) = \sum_{k=2}^{N}\sum_{j=2}^{L} \beta_{kj} e^{\sqrt{\lambda_{kj}}x} \mathbf{v}_{kj} + \sum_{k=2}^{N}\sum_{j=2}^{L} \overline{\beta}_{kj} e^{-\sqrt{\lambda_{kj}}x} \overline{\mathbf{v}}_{kj}, \tag{30}$$

where λ_{kj} and $\mathbf{v}_{kj}$ represent an eigenvalues and eigen vectors of equation (29). Noticeably, the dimension of the matrix in (29) is $(N-1)\times(L-1)$ as shown in Figure 2(b). The coefficients β_{kj} and $\overline{\beta}_{kj}$ are to be determined by $2(N-1)\times(L-1)$ boundary conditions at $x = -1$ and 1 when $y = y_k$ and $z = z_j$ in (19).

Example 1. For illustration, we first consider the following boundary conditions

$u = 0$ for $y = 0,1$,

$u = \sin \pi y$ for $x = 0$ and $u = e^{\pi} \sin \pi y$ for $x = 1$.

The analytical solution is given $u^* = e^{\pi x}\sin \pi y$. The average error ε between the numerical solution u and the analytical solution u^* is defined as

$$\varepsilon = \frac{1}{N_\varepsilon}\sum_{i=1}^{N_\varepsilon}\left|u_i - u_i^*\right|, \tag{31}$$

where N_ε is the number of testing points in the domain. The eigenvalues and average errors are presented in Table 1 for the different number of the integral line N along the y axis. It indicates that the average error is around 10^{-N}. Figure 3 shows the numerical and analytical solutions $u(x,1/2)$ along the x axis with the different number of integral line (end). The average relative error are 11.3.% while $N = 2$ and 0.28% while $N = 4$.

Table 1. Eigenvalues and relative errors versus the number of collocation point N.

N	$\sqrt{\lambda_1}$	$\sqrt{\lambda_2}$	$\sqrt{\lambda_3}$	$\sqrt{\lambda_4}$	$\sqrt{\lambda_5}$	$\sqrt{\lambda_6}$	$\sqrt{\lambda_7}$	ε
4	3.1343	6.9282	8.8417	--	--	--	--	5.7145E-04
6	3.1416	6.2860	9.1289	16.0982	17.2856	--	--	2.5100E-06
8	3.1416	6.2833	9.4203	12.7320	14.8290	28.3975	29.2829	1.8713E-08

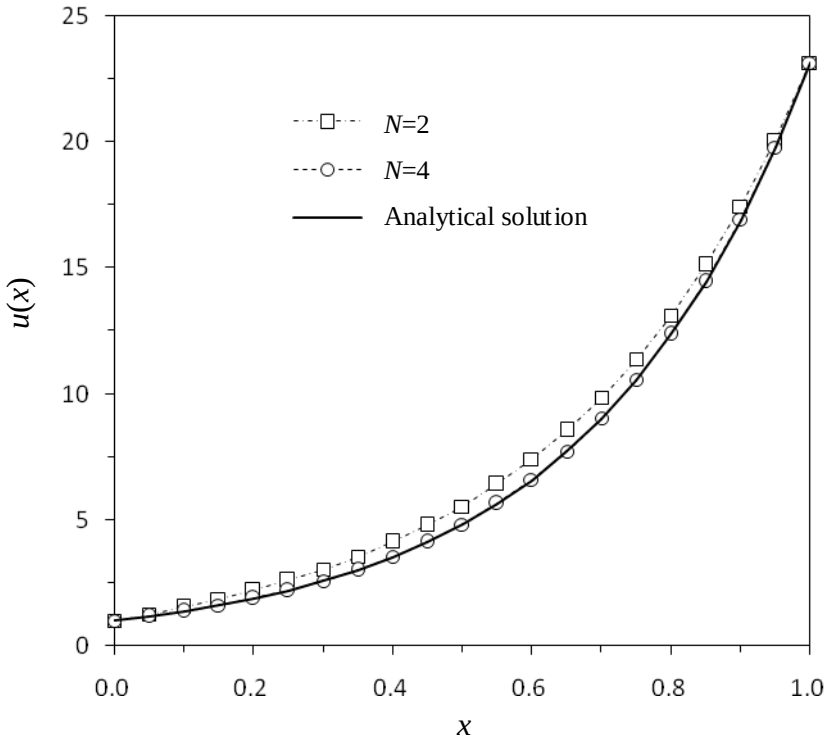

Figure 3. Distribution of temperature along $y = 0.5$ with the different number of the line.

Example 2. Consider the following boundary conditions [25]

$u = 100,\ \ y = 0$ (botom) and $u = 500,\ \ y = b$ (top),

$u = 100,\ \ x = 0$ and $x = a$ (sides),

where *a* and *b* are chosen as one unit. From the ordinary differential equation, one has

$$\frac{d^2 u_k}{dx^2} + \sum_{n=2}^{N} \frac{d^2 N_n(y_k)}{dy^2} u_n(x) = -\frac{d^2 N_1(y_k)}{dy^2} T_{side} - \frac{d^2 N_{N+1}(y_k)}{dy^2} T_{top} = b_k \text{(constant)},$$

$$k = 2,...., N. \tag{32}$$

As b_k are constants for each line, a particular solution u_k^p in (32) must be constant which can be determined from (32)

$$\mathbf{K}\mathbf{u}^p = \mathbf{b}, \tag{33}$$

in which $K_{kn} = \dfrac{d^2 N_n(y_k)}{dy^2}$. Then, the solution of Eq.(32) can be written, in vector form, as

$$\mathbf{u}(x) = \sum_{k=2}^{N-1} \beta_k e^{\sqrt{\lambda_k} x} \mathbf{v}_k + \sum_{k=2}^{N-1} \overline{\beta}_k e^{-\sqrt{\lambda_k} x} \overline{\mathbf{v}}_k + \mathbf{u}^p. \tag{34}$$

The analytical solution can be obtained [12]

$$u^*(x, y) = \frac{2\left(T_{top} - T_{side}\right)}{\pi} \sum_{n=1}^{\infty} \frac{(-1)^{n+1} + 1}{n} \sin\frac{n\pi x}{a} \times \frac{\sinh\dfrac{n\pi y}{a}}{\sinh\dfrac{n\pi b}{a}} + T_{side}. \tag{35}$$

The relative average error ε is defined as

$$\varepsilon = \frac{1}{N_\varepsilon} \sum_{i=1}^{N_\varepsilon} \left|u_i - u_i^*\right| / \left|u_i^*\right|. \tag{36}$$

The average relative errors are presented in Table 2 versus the number of uniformly distributed node *N* along the *y* axis. Excellent accuracy and convergence with semi-analytical solution can be seen from this table.

Table 2. Average relative errors.

N	ε
2	5.4343E-02
4	5.4811E-03
6	1.0135E-03
8	2.4065E-04
10	6.7325E-05

Example 3. Consider three dimensional Laplace equation in the domain Ω of $[0,1]^3$ with following boundary conditions

$u = 0$ for $y = 0,\ 1,$

$u = 0,$ for $z = 0,\ 1,$

$u = \sin \pi y \sin \pi z$ for $x = 0$ and $u = e^{\sqrt{2}\pi} \sin \pi y \sin \pi z$ for $x = 1.$

The analytical solution is $u^* = e^{\sqrt{2}\pi x} \sin \pi y \sin \pi z$. The relative average error ε between the analytical solution u and the computed solution u^* is defined in (36), where N_ε is the number of nodes in total $(N-1)(L-1)$ as shown in Figure 2(b). The eigenvalues and relative average errors are presented in Table 3 and Table 4 respectively versus the different number of collocations N along the y axis and L along the z-axis. Finite lines are collocated in the plane yoz $(\eta o \varsigma)$ along the x-axis and shown in Figure 4 when $N = 8$ and $L = 6$. To avoid the double roots of the eigenvalue, the numbers N and L should be selected as different values. Same again, very accurate solutions can be obtained even with few integral lines.

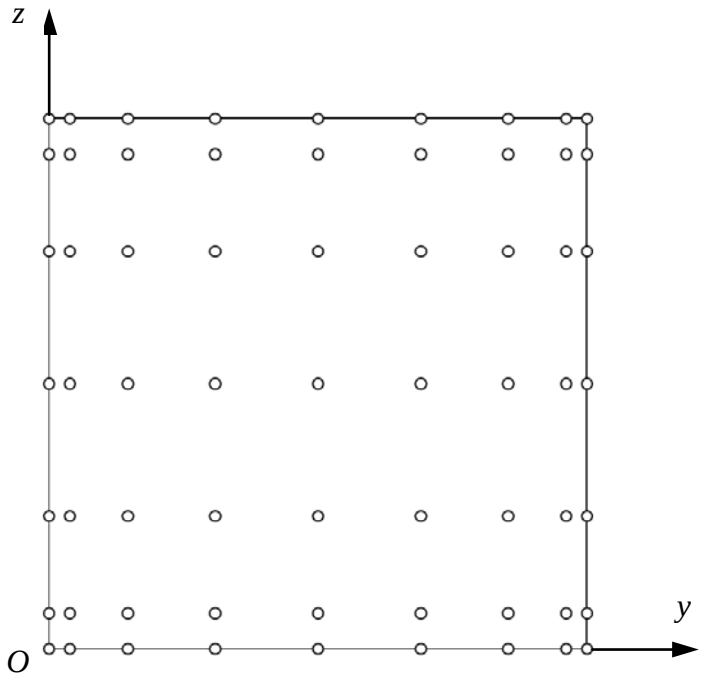

Figure 4. Distribution of the ends of integral lines in the plane of *yoz* for a three-dimensional problem.

Table 3. Eigenvalues with different nodes distributions.

(N,L)	$\sqrt{\lambda_1}$	$\sqrt{\lambda_2}$	$\sqrt{\lambda_3}$	$\sqrt{\lambda_4}$	$\sqrt{\lambda_5}$	$\sqrt{\lambda_6}$	$\sqrt{\lambda_7}$	$\sqrt{\lambda_8}$	$\sqrt{\lambda_9}$	$\sqrt{\lambda_{10}}$	$\sqrt{\lambda_{11}}$	$\sqrt{\lambda_{12}}$
(2, 1)	4.320	6.325	--	--	--	--	--	--	--	--	--	--
(3, 2)	4.527	6.467	7.659	8.944	9.426	10.496	--	--	--	--	--	--
(4, 3)	4.437	6.944	7.607	9.295	9.383	10.797	11.591	13.032	13.135	14.238	14.422	15.433

Table 4. Average errors with node densities.

N	L	ε
2	1	3.0008E-01
3	2	1.2701E-01
4	3	6.5856E-03
5	4	1.6051E-03
6	5	7.3520E-05
7	6	1.2231E-05
8	7	3.4916E-07

4. Numerical strategies for the ordinary differential equation

In order to solve an ordinary differential equation with variable coefficients *A, B, C, D* and *E* in (18), a numerical approach should be considered.

4.1 Finite different method

The finite difference method is the simplest method among the numerical approaches. Consider the approximations [26]

$$\frac{du}{d\xi} \approx \frac{u^{(i+1)} - u^{(i-1)}}{2\Delta}, \ \frac{d^2u}{d\xi^2} \approx \frac{u^{(i+1)} - 2u^{(i)} + u^{(i-1)}}{\Delta^2}. \tag{37}$$

Substituting (37) into (18) yields for a straight line *ab* ($\eta = \eta_k$) shown in Figure 1(a)

$$\frac{u_k^{(i+1)} - 2u_k^{(i)} + u_k^{(i-1)}}{\Delta^2} + A(\xi_i, \eta_k)\frac{u_k^{(i+1)} - u_k^{(i-1)}}{2\Delta} + B(\xi_i, \eta_k)\sum_{n=1}^{N+1}\frac{dN_n(\eta_k)}{d\eta}u_n^{(i)} +$$

$$C(\xi_i, \eta_k)\sum_{n=1}^{N+1}\frac{dN_n(\eta_k)}{d\eta}\frac{u_n^{(i+1)} - u_n^{(i-1)}}{2\Delta} + D(\xi_i, \eta_k)\sum_{n=1}^{N+1}\frac{d^2N_n(\eta_k)}{d\eta^2}u_n^{(i)} = Eb(\xi_i, \eta_k)$$

$$k = 2,..., N, i = 2,..., M\ . \tag{38}$$

Considering boundary conditions in (10), we can determine all nodal values $u_k^{(i)}$, $k = 1,2,..., N+1;\ i = 1,2,..., L+1$ by solving linear algebraic equations from (38).

4.2 Finite line integration method

By introducing the Direct Interation Method, the different order integral matrix $\mathbf{H}^{(1)}$ and $\mathbf{H}^{(2)}$ can be evaluated by the use of the Lagrange interpolation [22]. The procedure is very simple as follows. Any function $f(\xi)$ is approximated by Lagrange series, in a different form, as

$$f(\xi)=\sum_{m=1}^{M+1} a_m \xi^{m-1}, \qquad -1\le\xi\le 1, \tag{39}$$

where the coefficient $\{a_{km}\}_{m=1}^{M+1}$ are defined by

$$\begin{bmatrix} 1 & \xi_1 & \xi_1^2 & \cdots & \xi_1^M \\ 1 & \xi_2 & \xi_2^2 & \cdots & \xi_2^M \\ \cdots & \cdots & \cdots & \cdots & \cdots \\ 1 & \xi_{M+1} & \xi_{M+1}^2 & \cdots & \xi_{M+1}^M \end{bmatrix} \begin{pmatrix} a_1 \\ a_2 \\ \cdots \\ a_{M+1} \end{pmatrix} = \begin{pmatrix} f_1 \\ f_2 \\ \cdots \\ f_{M+1} \end{pmatrix} \quad \text{or} \quad \mathbf{Aa}=\mathbf{f}\,. \tag{40}$$

Then, one has

$$\mathbf{a}=\mathbf{A}^{-1}\mathbf{f}\,. \tag{41}$$

Therefore, one has single and double layers integrations

$$U^{(1)}(\xi)=\int f(\xi)d\xi=\sum_{m=1}^{M+1}\frac{a_m}{m}\xi^m, \tag{42}$$

$$U^{(2)}(\xi)=\int\int f(\xi)d\xi d\xi=\sum_{m=1}^{M+1}\frac{a_m}{m(m+1)}\xi^{m+1} \qquad -1\le\xi\le 1. \tag{43}$$

If $M+1$ collocation points are selected either uniformly or non-uniformly in (13) and (14), the indefinite integrals can be arranged in matrix form, in terms of the nodal values, as

$$\mathbf{U}^{(1)}=\mathbf{H}^{(1)}\mathbf{f}\,,\ \mathbf{U}^{(2)}=\mathbf{H}^{(2)}\mathbf{f}\,. \tag{44}$$

The dimension of $\mathbf{H}^{(1)}$ and $\mathbf{H}^{(2)}$ are $(M+1)\times(M+1)$ matrices respectively. Consider a line $\eta=\eta_k$ shown in Figure 2(a), integrating over both sides of equation (18) gives

$$\frac{du_k}{d\xi}+Au_k-\int\frac{dA}{d\xi}u_k d\xi+\sum_{n=1}^{N+1}\frac{dN_n(\eta_k)}{d\eta}\int Bu_n(\xi)d\xi+\sum_{n=1}^{N+1}\frac{dN_n(\eta_k)}{d\eta}\left[Cu_n(\xi)-\int\frac{dC(\xi)}{d\xi}u_n d\xi\right]$$

$$+\sum_{n=1}^{N+1}\frac{d^2N_n(\eta_k)}{d\eta^2}\int Du_n d\xi=\int Eb(\xi,\eta_k)d\xi+c_k \qquad k=2,....,N. \tag{45}$$

Taking integration again over the equation above, one has

$$u_k(\xi)+\int Au_k d\xi-\int\int\frac{dA}{d\xi}u_k d\xi d\xi+\sum_{n=1}^{N+1}\frac{dN_n(\eta_k)}{d\eta}\int\int Bu_n d\xi d\xi+\sum_{n=1}^{N+1}\frac{dN_n(\eta_k)}{d\eta}\times$$
$$\left[\int Cu_n(\xi)d\xi-\int\int\frac{dC(\xi)}{d\xi}u_n d\xi d\xi\right]+\sum_{n=1}^{N+1}\frac{d^2N_n(\eta_k)}{d\eta^2}\int\int Du_n d\xi d\xi=\int\int Eb(\xi,\eta_k)d\xi d\xi+c_k\xi+d_k$$
$$k=2,....,N \tag{46}$$

By introducing integral matrix, (12) and (13) can be written in a matrix form

$$\frac{\partial\mathbf{u}_k}{\partial\xi}+\mathbf{u}_k-\mathbf{H}^{(1)}\mathbf{A}_{,\xi}\mathbf{u}_k+\sum_{n=1}^{N+1}\frac{dN_n(\eta_k)}{d\eta}\mathbf{H}^{(1)}\mathbf{B}\mathbf{u}_n+\sum_{n=1}^{N+1}\frac{dN_n(\eta_k)}{d\eta}\times$$
$$\left[\mathbf{C}\mathbf{u}_n-\mathbf{H}^{(1)}\mathbf{C}_{,\xi}\mathbf{u}_n\right]+\sum_{n=1}^{N+1}\frac{d^2N_n(\eta_k)}{d\eta^2}\mathbf{H}^{(1)}\mathbf{D}\mathbf{u}_n=\mathbf{H}^{(1)}\mathbf{E}\mathbf{b}_k+c_k \qquad k=2,....,N \tag{47}$$

and

$$\mathbf{u}_k+\mathbf{H}^{(1)}\mathbf{u}_k-\mathbf{H}^{(2)}\mathbf{A}_{,\xi}\mathbf{u}_k+\sum_{n=1}^{N+1}\frac{dN_n(\eta_k)}{d\eta}\mathbf{H}^{(2)}\mathbf{B}\mathbf{u}_n+\sum_{n=1}^{N+1}\frac{dN_n(\eta_k)}{d\eta}\times$$
$$\left[\mathbf{H}^{(1)}\mathbf{C}\mathbf{u}_n-\mathbf{H}^{(2)}\mathbf{C}_{,\xi}\mathbf{u}_n\right]+\sum_{n=1}^{N+1}\frac{d^2N_n(\eta_k)}{d\eta^2}\mathbf{H}^{(2)}\mathbf{D}\mathbf{u}_n=\mathbf{H}^{(2)}\mathbf{E}\mathbf{b}_k+c_k\boldsymbol{\xi}+d_k\mathbf{i} \qquad k=2,....,N, \tag{48}$$

where $\mathbf{u}_k=\{u_{km}\}_{m=1}^{M+1}$ is the vector of potential for k-th curve, $\boldsymbol{\xi}=(\xi_1,\xi_2,...,\xi_{M+1})^T$, a unit vector $\mathbf{i}=\{1,1,...,1\}^T$ and diagonal matrices

$$\mathbf{A}_{,\xi}=\begin{pmatrix}\frac{\partial A(\xi_1)}{\partial\xi} & 0 & 0 & 0\\ 0 & \frac{\partial A(\xi_2)}{\partial\xi} & 0 & 0\\ .. & .. & .. & ..\\ 0 & 0 & 0 & \frac{\partial A(\xi_{M+1})}{\partial\xi}\end{pmatrix},\ \mathbf{C}_{,\xi}=\begin{pmatrix}\frac{\partial C(\xi_1)}{\partial\xi} & 0 & 0 & 0\\ 0 & \frac{\partial C(\xi_2)}{\partial\xi} & 0 & 0\\ .. & .. & .. & ..\\ 0 & 0 & 0 & \frac{\partial C(\xi_{M+1})}{\partial\xi}\end{pmatrix}. \tag{49}$$

Combined with the boundary conditions on four surfaces in (10), the nodal values of $\mathbf{u}_k$ and the integral constants (c_k,d_k) associated with each integral line can be obtained.

Example 4. Consider a two dimensional Laplace equation in the domain as shown in Figure 3. Boundary conditions are specified as

$u = 0 \quad y = 0$ (bottom) and $y = (1 + x^2)/2$ (top)

$q = \pi y(y - 1/2) \quad x = 0$ (left-hand side)

$u = 0 \quad x = 1$ (right-hand side)

As a flux density is given on the left-hand side, i.e. $\xi = \xi_1$, where $n_x = -1, n_y = 0$. The coordinate transformation gives

$$q(\eta_k) = \frac{du}{dn} = \frac{du}{dx} n_x + \frac{du}{dy} n_y = -\alpha_{11} \frac{\partial u}{\partial \xi} - \alpha_{12} \frac{\partial u}{\partial \eta}$$
$$= -\alpha_{11} \sum_{m=1}^{M+1} \frac{\partial M_m(\xi_1)}{\partial \xi} u_{km} - \alpha_{12} \sum_{n=1}^{N+1} \frac{\partial N_n(\eta_k)}{\partial \eta} u_{n1}. \tag{50}$$

The analytical solution is assumed as

$$u^* = y\left(y - (1 + x^2)/2\right)\sin \pi x$$

with the body force term consequently

$$b(x, y) = [2 - y - \pi^2 y(y - (1 + x^2)/2]\sin \pi x - 2\pi xy \cos \pi x .$$

The mapping of the boundary and collocation points distribution are shown in Figure 5. The joints of the two axes i.e. (ξ_m, η_n), $m = 1,2,...,M+1; n = 1,2,...,N+1$, are locations of collocation point both in the physical domain and mapped domain, where $M = N = 5$. To observe the degree of accuracy of DIM proposed in this paper, the average errors of the temperature of the nodal value located in the domain both by FDM and DIM are shown in Table 4. The average errors of temperature are about 1% for FDM and 2% for DIM if $N = 3$.However, the degree of accuracy is improved significantly for DIM with a larger number of nodes. It has been observed that the numerical solution becomes unstable and divergence while $M \geq 15, N \geq 15$. It is because the interpolation with Lagrange series in (39) becomes unstable. Table 4 shows that the degree of accuracy with DIM is much higher than that with FDM when $N > 4$.

Table 4. Average errors for various node numbers

$(N = L)$	FDM	DIM
3	9.9765E-03	2.1762E-02
4	3.1432E-03	3.2138E-03
5	1.5730E-03	1.2489E-04
6	9.1827E-04	1.7402E-04
7	6.0000E-04	3.1564E-05

8	4. 1803E-04	1. 4186E-06
9	3. 0992E-04	1. 0529E-06
10	2. 3833E-04	1. 2859E-07
11	1. 8871E-04	1. 5401E-08

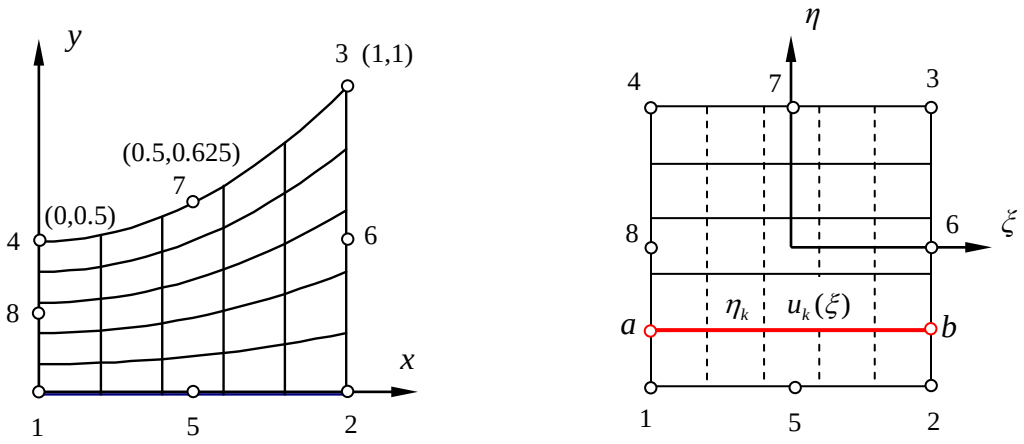

Figure 5. A two-dimensional nozzle: (a) real domain with finite lines; (b) transformed domain.

5. Time dependence problem

In the dynamic engineering, all physical values are time dependent. Apart from the dimension of geometry, time is a new extra dimension. Consider the two-dimensional wave equation as following

$$\begin{aligned} &\frac{\partial^2 u}{\partial x^2}+\frac{\partial^2 u}{\partial y^2}-\frac{1}{c^2}\frac{\partial^2 u}{\partial t^2}-\alpha\frac{\partial u}{\partial t}=f(x,y,t) && (x,y)\in\Omega,\ t>0,\\ &\frac{\partial u(x,y,0)}{\partial t}=v_0(x,y),\quad u(x,y,0)=u_0(x,y) && (x,y)\in\Omega,\ t=0,\\ &u(x,y,t)=g(x,y,t) && (x,y)\in\partial\Omega,\ t>0, \end{aligned} \tag{51}$$

where u is generally referred to as the transversal displacement of a membrane in mechanical engineering, f is body force, c is the propagation velocity, α the damping factor. In addition, v_0 and u_0 are given initial displacement and velocity in the domain, and g the boundary value. Applying the Laplace transformation on equation (51) gives

$$\frac{\partial^2 \tilde{u}}{\partial x^2}+\frac{\partial^2 \tilde{u}}{\partial y^2}-s\left(\frac{s}{c^2}+\alpha\right)\tilde{u}=\tilde{f}(x,y,s)+\frac{1}{c^2}[su_0+v_0]+\alpha u_0 \quad (x,y)\in\Omega,$$
$$\tilde{u}(x,y,s)=\tilde{g}(x,y,s), \quad (x,y)\in\partial\Omega, \tag{52}$$

where *s* denotes the Laplace transform parameter. By using DIM, one has system equation in matrix form (51)

$$\tilde{\mathbf{u}}_k+\mathbf{H}^{(1)}\tilde{\mathbf{u}}_k-\mathbf{H}^{(2)}\mathbf{A}_{,\xi}\tilde{\mathbf{u}}_k+\sum_{i=1}^{N}\frac{dN_i(\eta_k)}{d\eta}\mathbf{H}^{(2)}\mathbf{B}\tilde{\mathbf{u}}_i+\sum_{i=1}^{N}\frac{dN_i(\eta_k)}{d\eta}\times\left[\mathbf{H}^{(1)}\mathbf{C}\tilde{\mathbf{u}}_i-\mathbf{H}^{(2)}\mathbf{C}_{,\xi}\tilde{\mathbf{u}}_i\right]$$
$$+\sum_{i=1}^{N}\frac{d^2N_i(\eta_k)}{d\eta^2}\mathbf{H}^{(2)}\mathbf{D}\tilde{\mathbf{u}}_i-s\left(\frac{s}{c^2}+\alpha\right)\mathbf{H}^{(2)}\mathbf{E}\tilde{\mathbf{u}}_k=\mathbf{H}^{(2)}\mathbf{E}\tilde{\mathbf{b}}_k+c_k\boldsymbol{\xi}+d_k\mathbf{i}, \tag{53}$$

where all variables with "~" are transformed functions in the Laplace space, $\tilde{b}(x,y,s)=\tilde{f}(x,y,s)+[su_0+v_0]/c^2+\alpha u_0$. All nodal values of the displacement can be obtained numerically in the Laplace space for each specified parameter s_k . Consider (*K*+1) samples in the transformation domin $s_k, k=0,1,...,K$, the transformed variables $\tilde{u}(x,y,s_k)$ are evaluated both by the FDM and the DIM. Finally, the inversion proposed by Durbin [27] is adopted and it gives

$$u(t)=\frac{2e^{\omega t/T}}{T}\left[-\frac{1}{2}\tilde{u}(\omega/T)+\sum_{k=0}^{K}\mathrm{Re}\left\{\tilde{u}\left(\omega/T+2k\pi i/T\right)e^{2k\pi i/T}\right\}\right], \tag{54}$$

where $\tilde{u}(s_k)$ denotes the transformed variable in the Laplace domain while the parameter of the Laplace transform is chosen as $s_k=(\omega+2k\pi i)/T \quad (i=\sqrt{-1})$. In the Durbin Laplace transform reverse method, there are two free parameters: ω and *T*. The selection of parameters *T* depends on the observing period in the time domain [28].

Consider a rectangular membrane under initial displacement over the entire domain as shown in Figure 1 $(0\le x\le a, 0\le y\le b)$. The initial displacement and velocity conditions are specified as [29]

$$u_0(x,y,0)=16Ux(a-x)y(b-y)/a^2b^2; \quad v_0(x,y,0)=0,$$

where *U* is maximum displacement at the centre of the plate. Considering the boundary condition for a simply supported plate, the general solution can be represented in the series form as

$$u=\sum_{m=1}^{\infty}\sum_{n=1}^{\infty}F_{mn}(t)\sin\frac{m\pi x}{a}\sin\frac{n\pi y}{b}, \quad m,n=1,2,3... , \tag{55}$$

where

$$F_{mn}(t) = B_1 e^{\beta_1 t} + B_2 e^{\beta_2 t}, \tag{56}$$

in which β_i $(i = 1,2)$ are two roots of the following equation

$$\beta^2 + c^2\alpha\beta + \lambda_{mn}^2 = 0, \tag{57}$$

where $\lambda_{mn} = c\pi\sqrt{m^2/a^2 + n^2/b^2}$. Then we have

$$\beta_{1,2} = \frac{-c^2\alpha \pm \sqrt{c^4\alpha^2 - 4\lambda_{mn}^2}}{2}. \tag{58}$$

The coefficients B_1 and B_2 in (56) are determined by the initial conditions. For example, if the initial conditions are given by

$$u(x, y, 0) = u_0(x, y), \quad \frac{\partial u(x, y, 0)}{\partial t} = 0. \tag{59}$$

Substituting (10) into (13) yields

$$B_1 + B_2 = B_{mn}, \quad \beta_1 B_1 + \beta_2 B_2 = 0, \tag{60}$$

where

$$B_{mn} = \frac{4}{ab}\int_0^a\int_0^b u_0(x, y)\sin\left(\frac{m\pi x}{a}\right)\sin\left(\frac{n\pi y}{b}\right)dydx \tag{61}$$

and therefore, the function

$$F_{mn}(t) = -\frac{\lambda_{mn}^2}{\sqrt{c^4\alpha^2 - 4\lambda_{mn}^2}}\left[\frac{e^{\beta_1 t}}{\beta_1} - \frac{e^{\beta_2 t}}{\beta_2}\right]B_{mn}. \tag{62}$$

If $\lambda_{mn} > c^2\alpha/2$, the function $F_{mn}(t)$ can be simplified as

$$F_{mn}(t) = -\frac{2\lambda^2 e^{-c^2\alpha t/2}}{\omega_{mn}}\mathrm{Im}\left[\frac{e^{i\omega_{mn}t/2}}{-c^2\alpha + i\omega_{mn}}\right]B_{mn}, \tag{63}$$

where $\omega_{mn} = \sqrt{4\lambda_{mn}^2 - c^4\alpha^2}$. If $\lambda_{mn} \le c^2\alpha/2$, the function $F_{mn}(t)$ takes

$$F_{mn}(t) = -\frac{2\lambda^2 e^{-c^2\alpha t/2}}{\omega_{mn}}\left[\frac{e^{\omega_{mn}t/2}}{-c^2\alpha + \omega_{mn}} - \frac{e^{-\omega_{mn}t/2}}{-c^2\alpha - \omega_{mn}}\right]B_{mn}. \tag{64}$$

For the Durbin's inversion method of Laplace transform, two free parameters are selected as $\omega = 5$ and $T = 40$. The number of the sample point in the Laplace transform space $K = 100$. The dimension of a rectangular membrane $a = b = 1$. The numerical solutions of the normalized

displacement *u/U* at the central point of the plate $(a/2, a/2)$ are shown in Figure 6 (a)(b) when the damping factor α is taken as 0 and 0.5 respectively. It has been noticed that at the very beginning of time, i.e. $t = 0$, there is a jump and the exact solution for the membrane displacement u should be $u(0) = [u(0^+) - u(0^-)]/2 = 0.5$. Figures 6(a)(b) shows the difference between the numerical solutions with FDM/DIM and analytical solution when $N = L = 6$. Clearly, the direct integration method is of higher accuracy than the finite difference method. The more accurate solution can be obtained using more lines (*N*) and collocation points (*M*) on each integration line. In addition, the free parameters have very small effect on the computational accuracy of the results.

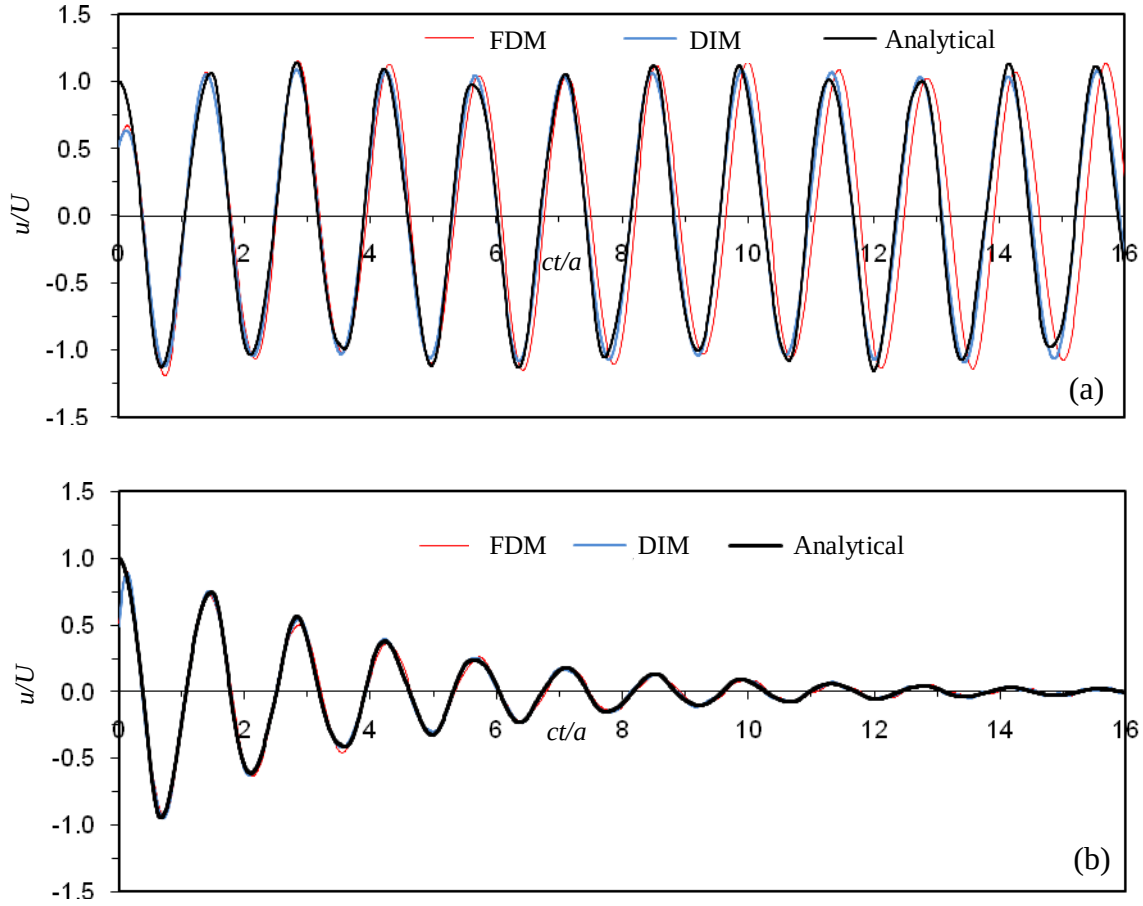

Figure 6. Normalised displacement *u/U* versus the normalised time *ct/a*: (a) without damping $(\alpha = 0)$; (b) with damping $(\alpha = 0.5)$.

6. Conclusion

A dimensional reduction method, the direct integration method, was proposed to solve the multi-dimensional partial differential equations numerically. By the mapping technique and Lagrange series interpolation, the general partial differential equation in the physical domain was transformed to a set of the ordinary differential equation in the normalized domain. A set of ordinary differential equations was solved by DIM proposed in this paper numerically with an excellent degree of accuracy when compared with the finite difference method. In DIM, the different orders of integration matrices were obtained easily with Lagrange series both for two and three-dimensional problems. Dynamic problems were studied in the Laplace transform domain and it has been shown that the DIM is an accurate algorithm. Although the simple case with one domain is considered in this paper, the DIM can be developed to the more complicated problem with smooth irregular domains such as amoeba-shape domain and large systems. In this case, subregion technique should be introduced. The proposed DIM can be extended to solve more complicated problems in engineering such as elasticity, elastoplasticity linear/nonlinear and fracture problems.

Acknowledgement

The work was supported partially by the National Natural Science Foundation of China (No:51704040, 51608055) and the Construction Project of Science and Technology of Ministry of Transport of the People's Republic of China (No:2015318825120).

References

[1] Y. Miyamoto, W.A. Kaysser, B.H. Rabin, A. Kawasaki, R.G. Ford, *Functionally Graded Materials; Design, Processing and Applications*, Kluwer Academic Publishers, Dordrecht, 1999.

[2] Zienkiewicz OC, Kelly DW, Bettess P. The coupling of the finite element method and boundary solution procedures. *Int. J. Numer. Methods Eng*. 1977; 11: 355-375.

[3] Brebbia C, Walker S. *Boundary element techniques in engineering*, Newnes Butterworths, London, England, 1980.

[4] Wood WL. On the finite element solution of an exterior boundary value problem. *Int. J. Numer. Methods Eng.* 1976; 10: 885-891.

[5] Lambert JD. *Numerical methods for ordinary differential systems: the initial value problem*. John Wiley & Sons, New York, 1991.

[6] J. Li, A.H-D. Cheng & C-S Chen, A comparing of efficiency and error convergence of multiquadric collocation method and finite element method, *Engng Analy with Boundary Elements*, 27, 251-257, 2003.

[7] M.A. Golgerg, C.S. Chen & S.R. Karur, Improved multiquadric approximation for partial differential equations, *Engng Analy with Boundary Elements*, 18, 9-17, 1996.

[8] R. L. Hardy, Multiquadric equations of topography and other irregular surface, J. Geophys. Res., 76, 1905-1915, 1971.

[9] Y.C. Hon & X.Z. Mao, A multiquadric interpolation method for solving initial value problems, *J. Scientific Computing*, 12, 51-55, 1997.

[10] Belytschko T, Lu YY, Gu L. Element-free Galerkin method. *Int. J. Numer. Methods Eng.*1994; 37: 229-256.

[11] Liu WK, Jun S, Zhang Y. Reproducing kernel particle methods. *Int. J. Numer. Methods Eng.* 1995; 20: 1081-1106.

[12] S.N. Atluri & T. Zhu, A new meshless local Peyrov-Galerkin (MLPG) approach to nonlinear problems in computational modelling and simulation, *Comput Model Simul Engng*, 3, 187-196, 1998.

[13] Sladek J., Sladek V., Zhang Ch. Transient heat conduction analysis in functionally graded materials by the meshless local boundary integral equation method. *Comput. Material Science* 2003; 28: 494-504.

[14] Sladek J., Sladek V., Krivacek J., Zhang Ch. (2003b) Local BIEM for transient heat conduction analysis in 3-D axisymmetric functionally graded solids. *Computational Mechanics* 2003; 32: 169-176.

[15] Nayroles B, Touzot G, Villon P. Generalizing the finite element method: diffuse approximation and diffuse elements. *Computational Mechanics* 1992; 10: 307-318.

[16] Song Ch, Wolf JP. The scaled boundary finite -element method-alias consistent infinitesimal finite-element cell method-for elastodynamics. *Computer Methods in Applied Mechanics and Engineering* 1997; 147:329–355.

[17] Song Ch, Wolf JP. The scaled boundary finite-element method-alias consistent infinitesimal finite-element cell method-for diffusion. *International Journal for Numerical Methods in Engineering* 1999; 45:1403–1431.

[18] Fan SC, Li SM, Yu GY. Dynamic fluid-structure interaction analysis using boundary-finite element method-finite element method. *Journal of Applied Mechanics* (ASME) 2005; 72:591–598.

[19] Lehmann L, Langer S, Clasen D. Scaled boundary finite element method for acoustics. *Journal of Computational Acoustics* 2006; 14:489–506.

[20] Liu JY, Lin G. Evaluation of stress intensity factors subjected to arbitrarily distributed tractions on crack surfaces. China Ocean Engineering 2007; 21:293–304.

[21] Wen PH, Hon YC, Li M, Korakianitis T. Finite integration method for partial differential equations. *Applied Mathematical Modelling* 2013;37(24):10092-10106.

[22] Wen PH, Chen CS, Hon YC, Li M. Finite integration method for solving multi-dimensional partial differential equations. *Applied Mathematical Modelling* 2013; 37(24):10092-10106.

[23] Li M, Hon YC, Korakianitis T, Wen PH. Finite integration method for nonlocal elastic bar under static and dynamic loads. *Engineering Analysis with Boundary Elements* 2013; 37(5):842-849.

[24] Lei M, Li, M. Wen PH and Bailey CG. Moving boundary analysis in heat conduction with multilayer composites by finite block method. *Engineering Analysis with Boundary Elements* 2018; 89:36-44.

[25] Roland W.L., Perumal, N., Kankanhalli, N. *Fundamentals of the Finite Element Method for Heat and Fluid Flow*. 2004 John Wiley & Sons Ltd, England.

[26] J.D. Lambert, *Numerical methods for ordinary differential systems* : the initial value problem, John Wiley & Sons, New York, 1991.

[27] Durbin, F., 1975. Numerical inversion of Laplace transforms: an efficient improvement to Dubner and Abate's method. *The Computer J*. 17, 371-376.

[28] Wen, P.H., Aliabadi, M.H. and Rooke, D.P., 1996. The influence of elastic waves on dynamic stress intensity factors (three dimensional problem), *Archive of Applied Mechanics*, 66(6), 385-384.

[29] Wen, P.H. and Chen, C.S. The method of particular solutions for solving scalar wave equations. *Int J. Numer. Meth.in Biomedical Engng*, 26 (12), 1878–1889, (2010).

Appendix

Firstly the first order partial differential of shape function with respect to normalized axes ξ and η are

$$\frac{\partial M_i}{\partial \xi}=\frac{\xi_i}{4}(1+\eta_i\eta)(2\xi_i\xi+\eta_i\eta),\ \frac{\partial M_i}{\partial \eta}=\frac{\eta_i}{4}(1+\xi_i\xi)(\xi_i\xi+2\eta_i\eta) \qquad \text{for } i=1,2,3,4 \tag{A1}$$

$$\frac{\partial M_i}{\partial \xi}=-\xi(1+\eta_i\eta),\ \frac{\partial M_i}{\partial \eta}=\frac{\eta_i}{2}(1-\xi^2) \qquad \text{for } i=5,7 \tag{A2}$$

$$\frac{\partial M_i}{\partial \xi}=\frac{\xi_i}{2}(1-\eta^2),\ \frac{\partial M_i}{\partial \eta}=-\eta(1+\xi_i\xi) \qquad \text{for } i=6,8 \tag{A3}$$

and their second order partial differential with respect to normalized axes ξ and η are

$$\frac{\partial^2 M_i}{\partial \xi^2}=\frac{\xi_i^2}{2}(1+\eta_i\eta),\ \frac{\partial^2 M_i}{\partial \xi\partial \eta}=\frac{\xi_i\eta_i}{4}(2\xi_i\xi+2\eta_i\eta+1),\ \frac{\partial^2 M_i}{\partial \eta^2}=\frac{\eta_i^2}{2}(1+\xi_i\xi) \quad \text{for } i=1,2,3,4 \tag{A4}$$

$$\frac{\partial^2 M_i}{\partial \xi^2}=-(1+\eta_i\eta),\ \frac{\partial^2 M_i}{\partial \xi\partial \eta}=-\eta_i\xi,\ \frac{\partial^2 M_i}{\partial \eta^2}=0 \quad \text{for } i=5,7 \tag{A5}$$

$$\frac{\partial^2 M_i}{\partial \xi^2}=0,\ \frac{\partial^2 M_i}{\partial \xi\partial \eta}=-\xi_i\eta,\ \frac{\partial^2 M_i}{\partial \eta^2}=-(1+\xi_i\xi) \quad \text{for } i=6,8 \tag{A6}$$

In (45) and (46), we need following high order partial differentials

$$\frac{\partial \alpha_{ij}}{\partial \xi},\frac{\partial \alpha_{ij}}{\partial \eta},\frac{\partial^2 \alpha_{ij}}{\partial \xi^2},\frac{\partial^2 \alpha_{ij}}{\partial \xi\partial \eta},\frac{\partial^2 \alpha_{ij}}{\partial \eta^2} \quad i,j=1,2, \tag{A7}$$

where

$$\alpha_{ij}=\frac{\beta_{ij}}{J},\ \ \beta_{11}=\frac{\partial y}{\partial \eta},\beta_{12}=-\frac{\partial y}{\partial \xi},\beta_{21}=-\frac{\partial x}{\partial \eta},\beta_{22}=\frac{\partial x}{\partial \xi},\ J=\beta_{11}\beta_{22}-\beta_{21}\beta_{12}. \tag{A8}$$

Then

$$\frac{\partial \alpha_{ij}}{\partial \xi}=\frac{1}{J^2}\left(J\frac{\partial \beta_{ij}}{\partial \xi}-\beta_{ij}\frac{\partial J}{\partial \xi}\right),\ \frac{\partial \alpha_{ij}}{\partial \eta}=\frac{1}{J^2}\left(J\frac{\partial \beta_{ij}}{\partial \eta}-\beta_{ij}\frac{\partial J}{\partial \eta}\right), \tag{A9}$$

$$\frac{\partial^2 \alpha_{ij}}{\partial \xi^2}=\frac{1}{J^3}\left[J^2\frac{\partial^2 \beta_{ij}}{\partial \xi^2}-2J\frac{\partial \beta_{ij}}{\partial \xi}\frac{\partial J}{\partial \xi}-J\beta_{ij}\frac{\partial^2 J}{\partial \xi^2}+2\beta_{ij}\left(\frac{\partial J}{\partial \xi}\right)^2\right], \tag{A10}$$

$$\frac{\partial^2 \alpha_{ij}}{\partial \xi \partial \eta} = \frac{1}{J^3}\left[J^2 \frac{\partial^2 \beta_{ij}}{\partial \xi \partial \eta} - J \frac{\partial \beta_{ij}}{\partial \xi}\frac{\partial J}{\partial \eta} - J \frac{\partial \beta_{ij}}{\partial \eta}\frac{\partial J}{\partial \xi} - J\beta_{ij}\frac{\partial^2 J}{\partial \xi \partial \eta} + 2\beta_{ij}\frac{\partial J}{\partial \xi}\frac{\partial J}{\partial \eta}\right]. \tag{A11}$$

It is not difficult to obtain the first order partial differential of $\partial A/\partial \xi$ and $\partial C/\partial \xi$. In addition, the partial differential of coordinate in β_{ij}

$$\frac{\partial x}{\partial \xi} = \sum_{k=1}^{8} \frac{\partial M_k}{\partial \xi} x_k, \ \frac{\partial y}{\partial \xi} = \sum_{k=1}^{8} \frac{\partial M_k}{\partial \xi} y_k . \tag{A12}$$